Lab on a Chip

Cite this: DOI: 10.1039/c1lc20511k

www.rsc.org/loc

PAPER

Demonstration of motionless Knudsen pump based micro-gas chromatography featuring micro-fabricated columns and on-column detectors

Jing Liu,[ac] Naveen K. Gupta,[bc] Kensall D. Wise,[bc] Yogesh B. Gianchandani*[bc] and Xudong Fan*[ac]

Received 13th June 2011, Accepted 29th July 2011
DOI: 10.1039/c1lc20511k

This paper reports the investigation of a micro-gas chromatography (μGC) system that utilizes an array of miniaturized motionless Knudsen pumps (KPs) as well as microfabricated separation columns and optical detectors. A prototype system was built to achieve a flow rate of 1 mL min^{-1} and 0.26 mL min^{-1} for helium and dry air, respectively, when they were used as carrier gas. This system was then employed to evaluate GC performance compromises and demonstrate the ability to separate and detect gas mixtures containing analytes of different volatilities and polarities. Furthermore, the use of pressure programming of the KP array was demonstrated to significantly shorten the analysis time while maintaining a high detection resolution. Using this method, we obtained a high resolution detection of 5 alkanes of different volatilities within 5 min. Finally, we successfully detected gas mixtures of various polarities using a tandem-column μGC configuration by installing two on-column optical detectors to obtain complementary chromatograms.

Introduction

In application arenas that range from environmental monitoring to oil exploration, and homeland security there is a significant need for highly sensitive, specific, and robust gas analysis systems that are able to detect/identify *in situ* the trace level of volatile organic compounds (VOCs) in real-time. Micro-gas chromatography (μGC) is particularly suited for analyzing VOC mixtures of arbitrary composition.[1–7] Typically, a μGC system consists of a preconcentrator for analyte sampling,[8–10] a short capillary column[11,12] or micro-fabricated column[3–6,13–18] for rapid VOC separation, one detector or more to detect separated analytes,[1,11,15,19–21] and one pump or more to provide carrier gas flow for sample delivery.[19] Significant progress has been made toward the miniaturization and performance improvement of each component of the μGC system, in particular, detectors[1,11,15,19,21,22] and separation columns.[3–6,11–18]

The progress in using new types of miniature pumps, however, has been modest. To date, diaphragm pumps[11,21,23] and turbo molecular pumps[24] have been integrated with various μGC systems. Although different in design details and pumping mechanisms, these pumps all rely on mechanical motion to provide the flow needed in μGC systems. The moving parts present challenges with reliability, and typically require lubrication and maintenance, making these unsuitable for extended deployment in remote locations or harsh environment. Additionally, miniaturization of mechanical pumps compromises performance, as frictional forces assume a dominant role.

In contrast, the Knudsen pump (KP) is a motionless pump based on thermal transpiration, which drives the flow of gas molecules from the cold end to the hot end within a narrow channel subjected to a temperature gradient.[25–30] In the long term, the KP has a number of potential advantages over the mechanical pump. First, the absence of moving parts results in enhanced reliability and maintenance-free operation exceeding 10^4 h of continuous operation, making these pumps attractive for operation in remote and inaccessible environments. Second, the absence of any noise or sound from these pumps is appealing for hospital environments or surveillance applications. Third, the KP's performance scales favorably with its size. In order to make the transpiration phenomenon significant in the KP, it is necessary for the channel diameter to be on the order of sub-micron or nanometre.

Although the thermal transpiration phenomenon was first studied back in 1879 and recognized as a promising technology for making motionless pumps, most of the KPs reported before early 2000s were operated at sub-atmospheric pressure due to the lack of appropriate materials or methods to form sufficiently small channels. The introduction of new materials with sub-micron channels and the advance of micro-fabrication technology have recently led to miniaturized KPs capable of operating at the atmospheric pressure and generating reasonably high pumping pressures.[26,31–33] However, flow rate and pressure have

[a]*Department of Biomedical Engineering, University of Michigan, 1101 Beal Avenue, Ann Arbor, Michigan, 48109, USA. E-mail: xsfan@umich.edu*
[b]*Department of Electrical Engineering and Computer Science, University of Michigan, 1301 Beal Avenue, Ann Arbor, Michigan, 48109, USA. E-mail: yogesh@umich.edu*
[c]*Engineering Research Center for Wireless Integrated Microsystems, University of Michigan, 1301 Beal Avenue, Ann Arbor, Michigan, 48109, USA*

remained as challenges, and the practical application of a miniature KP to μGC systems has not been reported prior to this effort.

In this paper, we report the integration of a KP array with a μGC system comprised of micro-fabricated GC columns and on-column optical detectors.[34] The KP array consisted of six KPs connected in series, with each KP element made of a mesoporous polymer having a high nano-channel density,[26,33] which can provide a sufficient flow rate (>0.1–1 mL min^{-1}) for the μGC system with either helium or dry air as the carrier gas rate. The capabilities of the KP driven μGC system to separate and detect gas mixtures containing analytes of different volatilities and polarities were demonstrated. The use of pressure programming of the KP array for improved VOC separation was shown to shorten the analysis time while maintaining a high chromatographic resolution. Increased separation capability was also achieved in a tandem-column μGC configuration by installing two on-column detectors at the end of the first and the second micro-fabricated columns, respectively, to obtain complementary chromatograms.

Experimental section

The KP-based μGC system included three integrated modules: a KP array to transport gas samples along the system, a micro-fabricated GC column to separate gas mixtures, and an optical on-column detector to detect analytes without any interruption to the flow. Fig. 1(A) and (B) illustrate the two μGC configurations tested, and Fig. 1(C) shows the measurement set-up. Each of the components in the system is discussed as follows.

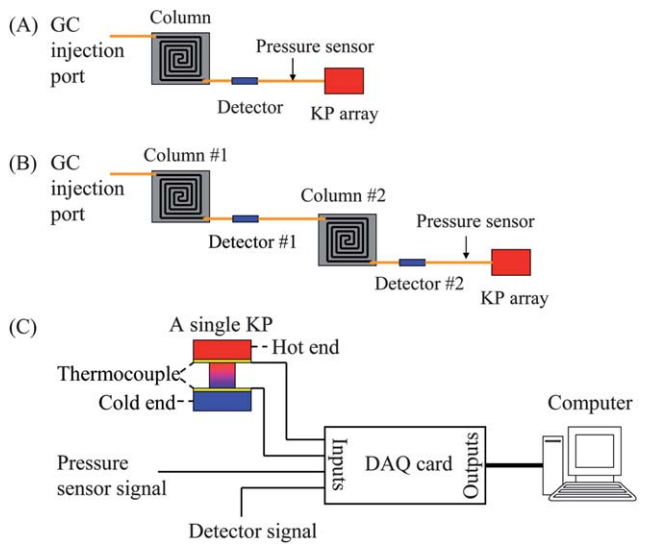

Fig. 1 (A) Schematic of the single-column system. It consisted of a 25 cm long micro-fabricated GC column coated with OV-1 and an on-column optical detector. (B) Schematic of the tandem-column system. It had two micro-fabricated GC columns. The first column was 50 cm long and was coated with OV-1, whereas the second column was 25 cm long and was coated with OV-215. Two on-column optical detectors were installed at the end of the first and the second column, respectively; (C) Schematic of the measurement set-up.

KP array

The KP array had six KP elements connected in series, which could provide a typical flow rate needed for the proposed μGC system. Each KP element was made of a mesoporous polymer membrane (diameter ≈11.5 mm, thickness ≈105 μm, pore diameter ≈25 nm, porosity ≈70%) sandwiched between a heated brass top and a passively cooled brass base. A single KP element is shown in Fig. 2(A), whereas series arrangement is illustrated in Fig. 2(B). The density of the mesoporous polymer membrane is approximately $10^{11}/cm^2$; this, along with a structure that is relatively free of defects, allow the relatively high flow rate necessary for the μGC operation.[26,33]

The temperature bias between the hot and cold brass plates results in the gas movement from the cold end to the hot end, as illustrated in Fig. 2(C). At equilibrium, the pressure ratio between the hot end (P_H) and the cold end (P_C) is ideally provided by the ratio of the square roots of the absolute temperature (T_H and T_C): $\frac{P_H}{P_C} = \frac{\sqrt{T_H}}{\sqrt{T_C}}$. In our experiment, a DC voltage supply ranging from 0 to75 V was applied on the KP array, which was equally allocated to each KP element to generate a temperature bias ranging from 38 to 96 K across each of the KP elements. The temperature bias was controlled and monitored in real-time by a customized LABVIEW™ program through thermocouples (Newport Electronics, 5SRTC-TT-K-40-36) attached to the hot and the cold end, respectively (as shown in Fig. 1(C)). The hydraulic connections between elements were made by clear Tygon tubes (inner diameter 0.18 mm).

Micro-fabricated GC column

The micro-fabricated GC column (see Fig. 3(A)) was fabricated by deep reactive ion etching of a 25 cm long double spiral channel

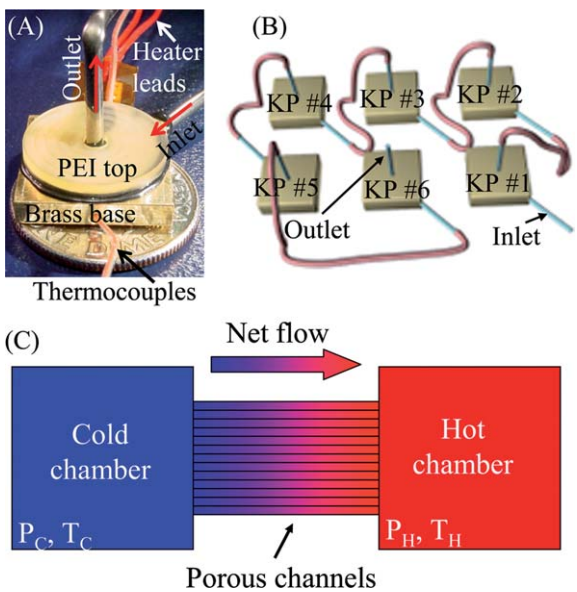

Fig. 2 (A) Photo of the KP element used as a building block for the KP array; (B) Diagram of the KP array that connected six single KP in series; (C) Schematic of a KP element that uses narrow channels (which can sustain free-molecular or transitional flow) subjected to a longitudinal temperature gradient to pump gas along the temperature gradient.

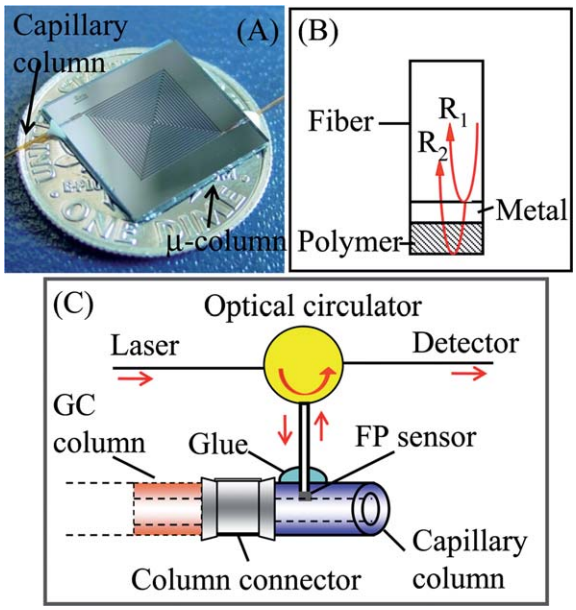

Fig. 3 (A) Photo of a 25 cm long silicon-glass micro-fabricated GC column; (B) Schematic of the FP sensing probe fabricated by sequentially coating the endface of a single mode optical fiber with metal and polymer. The two optical beams (R_1 and R_2) were reflected by the metal layer and polymer-air interface to form the interference spectrum. In our experiment, approximately 15 nm thick gold and 2 μm thick polydimethylsiloxane were used; (C) Schematic of the on-column optical detector assembled by inserting the FP sensing probe into a fused-silica capillary. Dimensions in (B) and (C) are not to scale.

into a silicon substrate, having a footprint of 1.1 cm by 1.1 cm.[15] A Pyrex 7740 glass cover plate was bonded anodically to the silicon substrate to seal the channel. The rectangular cross section of the channel was 150 μm wide and 240 μm deep. The connection of the micro-fabricated column to other components was made by inserting short conventional GC columns (inner diameter 100 μm, outer diameter 245 μm) to its inlet and outlet ports (245 μm wide and 245 μm deep).

Columns micro-fabricated for this study were coated with non-polar polymer of OV-1 or polar polymer of OV-215. The coating procedure included four steps.[18,35] (1) The non-polar coating solution was prepared by dissolving 22.3 mg OV-1 and 0.2 mg dicumyl peroxide in a 6 mL mixture of 1 : 1 (v:v) pentane and dichloromethane, whereas the polar coating solution was prepared by dissolving 20 mg OV-215 and 0.2 mg dicumyl peroxide in a 5 mL mixture of 1 : 4 (v:v) ether and ether acetate; (2) The micro-fabricated channel was filled with coating solution and held for 5 min; (3) The solvent was evaporated from one end of the column by a vacuum pump while the other end was sealed with a septum; (4) The polymer coating was cross-linked to the inner wall of the column by ramping the column temperature from 160 °C to 180 °C at a rate of 0.2 °C min^{-1} and staying at 180 °C for one hour. The resultant column coating had a uniform thickness of around 200 nm.

Optical on-column detector

The fabrication and assembly methods of the optical on-column detector (shown in Fig. 3(B) and (C)) were previously reported.[36,37] Briefly, the Fabry-Pérot (FP) based sensing probe (see Fig. 3(B)) was fabricated by sequentially depositing a thin layer of metal (such as gold and silver, 15 nm thick) and a layer of sensing polymer (such as polydimethylsiloxane and polyethylene glycol) on the end-face of a single mode optical fiber. The FP sensing probe was then assembled into a detector module by inserting it into a hole (approximately 160 μm in diameter) drilled on the wall of a short fused silica capillary (shown in Fig. 3 (C)), which can be easily connected to conventional GC columns through a press tight column connector from Restek (part# 484244). A 1550 nm tunable diode laser was coupled into the FP sensing probe through an optical circulator. The incident light partially reflected at the metal layer and polymer-air interface, generating an interference spectrum. By fixing the laser wavelength near the quadrature point around 1550 nm, the interference shifting caused by the polymer-analyte interaction can be converted to the intensity change of the reflected light; this was monitored by a photo-detector at the output port of the optical circulator. A customized LABVIEW™ program was used to monitor the signal change in real-time, and the data was recorded at a rate of 20 Hz.

The use of the optical on-column detector has several unique merits for the KP driven μGC system. First, the on-column detector does not interrupt the flow, which allows the KP to work in either pushing or pulling mode without involving any complicated connectors and valves, which potentially provides more flexibility and simplicity to the system fluidic design. Second, the on-column detector does not contribute any additional dead volume, and therefore, is particularly attractive to work under the low flow rate provided by current KP without degrading the system resolution. Finally, on-column detection technology can increase the detection specificity of the μGC system by integrating multiple detectors tailored for detecting different gas species. It can also be installed between two GC columns in the tandem-column μGC configuration (see Fig. 1(B)) to provide complementary chromatograms for higher chromatographic resolution, as discussed below.

Experimental set-up

Two μGC configurations were built to characterize the performance of the KP array, as illustrated in Fig. 1(A) and (B). For the single-column configuration (see Fig. 1(A)), an optical on-column detector was connected to the injection port installed on a Varian 3800 GC through a 25 cm long micro-fabricated column coated with OV-1. For the tandem-column configuration (see Fig. 1(B)), the first optical on-column detector was installed at the end of a 50 cm long micro-fabricated column coated with OV-1, and the second detector was installed at the end of a 25 cm long micro-fabricated column coated with OV-215. The columns were kept isothermally at room temperature during the experiments in this study. The KP array was installed at the downstream end of both configurations to pull the carrier gas and analytes through the whole system. A pressure sensor (Motorola, Inc. MPX2053DP) was installed to monitor the pressure on-column. Gas samples extracted from the head space of each sample container by a solid phase microextractor (SPME) was injected through the injection port. The temperature of the injection port was kept at 200 °C and its head pressure was set to

zero to prevent inadvertent flow from it. Either ultrahigh purity helium or dry air was used as the carrier gas.

Results and discussion

Single-column configuration

A gas mixture composing of pentane, heptane, octane, decane, and undecane was used to test the separation and detection capability of the KP-based single-column μGC system. Fig. 4 shows the separation chromatograms obtained at two different KP pumping pressures. A temperature bias of 84 K applied across each element of the KP array generates a pumping pressure of 20.6 kPa (and a helium flow rate of 1 mL min^{-1}), which unambiguously demonstrates the feasibility of using KP in a μGC system. In this effort, a rapid detection was completed within around 4 min, with a high resolution between heavy analytes of undecane and decane. However, the three light analytes of pentane, heptane, and octane were eluted out close to each other, making them nearly indiscernible. Another typical chromatogram was obtained with a lower flow rate (0.55 mL min^{-1}) by lowering the temperature bias across each of the KP elements to 38 K. This reduced the pumping pressure to 10.5 kPa, which allowed us to easily separate the three light analytes. However, this increased resolution was achieved at the expense of the overall analysis time. As shown in Fig. 4, the elution of heavy analytes was significantly slowed down, resulting in an analysis time of around 7 min.

In order to obtain superior resolution of this set of analytes without sacrificing the detection speed, simple pressure programming was used to modulate the pumping of the KP array during the analysis. A low pumping pressure of 10.5 kPa was applied at the beginning of the test to obtain high resolution for the light analytes. After the elution of the three light analytes, the pumping pressure was increased to 20.6 kPa to accelerate the elution of heavy analytes. In the resultant chromatogram, as illustrated in Fig. 5, the light analytes were eluted at 11.1 s, 16.7 s, and 27.4 s, respectively, and heavy analytes eluted out within 5 min. The inset of Fig. 5 shows the temperature measured at the hot end and the cold end of a single KP element. The pressure

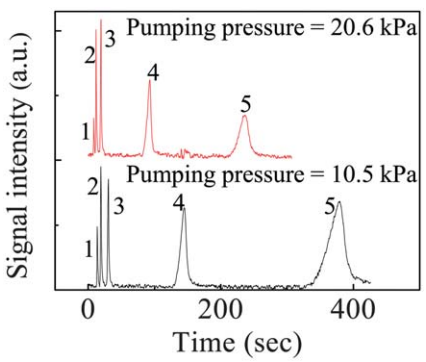

Fig. 4 Chromatograms obtained from single-column configuration when the pumping pressure was maintained at 20.6 kPa (corresponding flow rate was 1 mL min^{-1}) and 10.5 kPa (corresponding flow rate was 0.55 mL min^{-1}). Helium was used as the carrier gas. Curves are vertically shifted for clarity. 1. pentane; 2. heptane; 3. octane; 4. decane; 5. undecane.

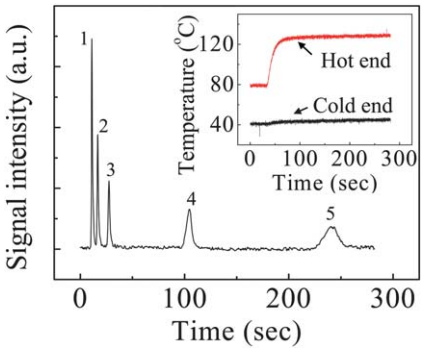

Fig. 5 Chromatogram obtained from single-column configuration with pressure programming of the KP array. The pumping pressure was set at 10.5 kPa at the beginning. After the elution of the third analyte, the pressure was increased to 20.6 kPa. Inset: Temperature recorded at the hot and cold end of a single KP element. 1. pentane; 2. heptane; 3. octane; 4. decane; 5. undecane.

programming of the KP array was implemented by simply modulating the temperature at the hot end of each KP element while allowing the cold end to remain in equilibrium with the environment. Multi-level pressure programming is certainly possible to analyze more complex gas mixtures and to optimize both system chromatographic resolution and detection speed.

We further tested the performance of the KP-based μGC system using dry air as the carrier gas. Employment of dry air for gas analysis is particularly appealing for μGC systems intended for use in environmental VOC monitoring. The use of inert carrier gas (such as helium and nitrogen) would require storage and replenishment adding to operation costs, and eliminating the possibility of use in remote and in accessible environments. In our experiment, the dry air was obtained by passing ambient air through a desiccant. Fig. 6 shows the separation chromatogram of five gas analytes: pentane, octane, decane, dimethyl methylphosphonate (DMMP) and undecane using the single-column μGC configuration when a temperature bias of 96 K was applied across each of the KP elements in the KP array. Note that because the average molecular diameter of air is larger than helium, the thermal transpiration driven flow rate decreased to 0.26 mL min^{-1}, compromising the chromatographic resolution

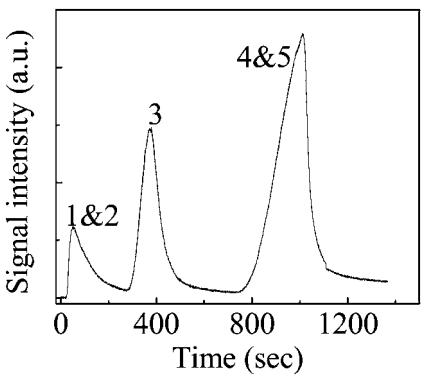

Fig. 6 Chromatogram obtained from single-column configuration. Dry air was used as the carrier gas with a flow rate of 0.26 mL/min. 1. pentane; 2. octane; 3. decane; 4. DMMP; 5. undecane.

and broadened peak width. Consequently, as shown in Fig. 6, pentane/octane and DMMP/undecane were co-eluted. This type of co-elution problem can be addressed, as described in the next section, using a tandem-column μGC configuration with two on-column detectors (see Fig. 1(B)) for better chromatographic resolution.

Tandem-column configuration

The tandem-column configuration has been used in μGC systems aimed to improve the μGC separation capability. It employs two columns with different coatings to first separate analytes by vapor pressure, followed by another separation by polarity.[38–40] In this study, two micro-fabricated GC columns with coatings of different polarities were used; two on-column detectors were installed at the end of the first and the second column, respectively (see Fig. 1(B)), to provide complementary chromatographs for enhanced chromatographic resolution.[37,41] Dry air was once again used as the carrier gas in this configuration. The temperature bias across each element of the KP array was maintained at 96 K, which resulted in a pumping pressure of 10 kPa and a flow rate of 0.14 mL/min. As shown in Fig. 7(A), although octane and *trans*-2-hexenal co-eluted after the first column because of the limited separation capability of the single column, all analytes were separated at the end of the tandem-column system. Note that the benefit of the tandem-column configuration may not be fully realized with the traditional end-column detector placed at the terminal end of the second column, as the analytes already separated after the first column may still co-elute after the second column,[37,41] which creates the same co-elution problem as in the single-column configuration. In contrast, installation of an additional on-column detector at the end of the first column allows us to monitor the separation from the first and the second column simultaneously, thus providing complementary chromatograms that significantly improve the analyte separation and identification capability of the μGC system. This point is well illustrated in Fig. 7(B), where the two complementary chromatograms were obtained from the first and the second on-column optical detectors, respectively. Although a co-elution of DMMP and undecane occurred after the second column, the complementary chromatogram obtained from the first detector was able to adequately separate the gas mixture.

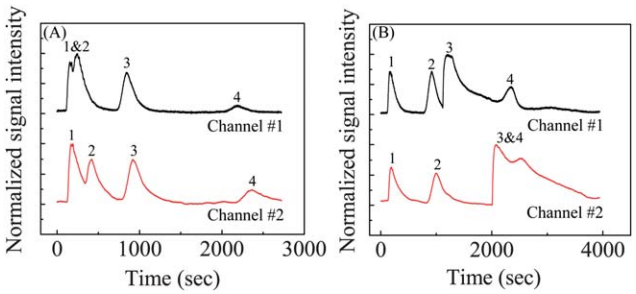

Fig. 7 Chromatograms obtained from the two optical detectors installed in the tandem-column configuration. Dry air was used as the carrier gas with a flow rate of 0.14 mL/min. All peaks are normalized to the highest peak in each chromatogram. Curves are vertically shifted for clarity. (A) At Channel #1 (placed after the first column), analyte #1 and #2 co-eluted, while at Channel #2 (placed after the second column) all analytes were resolved. 1. octane; 2. *trans*-2-hexenal; 3. decane; 4. undecane. (B) At Channel #1, all analytes were resolved, while at Channel #2 analyte #3 and #4 co-eluted. 1. octane; 2. decane; 3. DMMP; 4. undecane.

Conclusion and future work

In this paper, we reported, for the first time, the integration of a KP array based μGC system featuring on-column optical detectors and the micro-fabricated GC column. Using helium and dry air as the carrier gas the system demonstrated both strong separation and detection of gas mixtures with various polarities and volatilities. Pressure programming of the KP array enhanced chromatographic resolution while shortening the analysis time. We also evaluated a tandem-column configuration utilizing two on-column optical detectors, which provided complementary chromatograms following each of the two micro-fabricated columns.

Future work will be directed at improving the performance of each component of the KP-based μGC system and optimizing the system configuration. For component improvement, the KP will be further miniaturized and designed to achieve a higher pumping pressure and flow rate. We will also implement the temperature programming capability of the micro-fabricated GC column, which, in combination with pressure programming, will greatly improve the system chromatographic resolution and shorten the analysis time. A preconcentrator will also be integrated on board to further scale down the size of the whole μGC system.

Acknowledgements

The authors would like to thank Katharine Beach for fabricating the separation columns and Robert Gordenker for discussions. This work was supported in part by the NSF under ECCS-1058710, IOS-0946735, and EEC-9986866.

References

1 S. C. Terry, J. H. Jerman and J. B. Angell, *IEEE Trans. Electron Devices*, 1979, **26**, 1880–1886.
2 J. B. Angell, S. C. Terry and P. W. Barth, *Sci. Am.*, 1983, **248**, 44–45.
3 C. M. Yu, M. Lucas, C. Koo, P. Stratton, T. DeLima and E. Behymer, in *ASME International Mechanical Engineering Congress and Exposition*, American Society of Mechanical Engineers, Anaheim, CA, USA, 1998, pp. 481–486.
4 E. S. Kolesar Jr. and R. R. Reston, *IEEE Trans. Compon., Packag. Manuf. Technol., Part B*, 1998, **21**, 324–328.
5 E. B. Overton, K. R. Carney, N. Roques and H. P. Dharmasena, *Field Anal. Chem. Technol.*, 2001, **5**, 97–105.
6 H.-S. Noh, P. J. Hesketh and G. C. Frye-Mason, *J. Microelectromech. Syst.*, 2002, **11**, 718–725.
7 Q. Y. Cai and E. T. Zellers, *Anal. Chem.*, 2002, **74**, 3533–3539.
8 W.-C. Tian, H. K. L. Chan, C.-J. Lu, S. W. Pang and E. T. Zellers, *J. Microelectromech. Syst.*, 2005, **14**, 498–507.
9 P. Ivanov, F. Blanco, I. Graia, N. Sabat, A. Ruiz, X. Vilanova, X. Correig, L. Fonseca, E. Figueras, J. Santander and C. Can, *Sens. Actuators, B*, 2007, **127**, 288–294.
10 F. Bender, N. Barié, G. Romoudis, A. Voigt and M. Rapp, *Sens. Actuators, B*, 2003, **93**, 135–141.
11 C.-J. Lu, J. Whiting, R. D. Sacks and E. T. Zellers, *Anal. Chem.*, 2003, **75**, 1400–1409.
12 E. J. Staples and S. Viswanathan, *IEEE Sens. J.*, 2005, **5**, 622–631.

13 G. Lambertus, A. Elstro, K. Sensening, J. Potkay, M. Agah, S. Scheuering, K. Wise, F. Dorman and R. Sacks, *Anal. Chem.*, 2004, **76**, 2629–2637.
14 L. Lorenzelli, A. Benvenuto, A. Adami, V. Guarnieri, B. Margesin, V. Mulloni and D. Vincenzi, *Biosens. Bioelectron.*, 2005, **20**, 1968–1976.
15 G. Lambertus and R. Sacks, *Anal. Chem.*, 2005, **77**, 2078–2084.
16 M. Stadermann, A. D. McBrady, B. Dick, V. R. Reid, A. Noy, R. E. Synovec and O. Bakajin, *Anal. Chem.*, 2006, **78**, 5639–5644.
17 S. Reidy, D. George, M. Agah and R. Sacks, *Anal. Chem.*, 2007, **79**, 2911–2917.
18 S. Reidy, G. Lambertus, J. Geece and R. Sacks, *Anal. Chem.*, 2006, **78**, 2623–2630.
19 P. R. Lewis, R. P. Manginell, D. R. Adkins, R. J. Kottenstette, D. R. Wheeler, S. S. Sokolowski, D. E. Trudell, J. E. Byrnes, M. Okandan, J. M. Bauer, R. G. Manley and G. C. Frye-Mason, *IEEE Sens. J.*, 2006, **6**, 784–794.
20 C.-J. Lu, W. H. Steinecker, W.-C. Tian, M. C. Oborny, J. M. Nichols, M. Agah, J. A. Potkay, H. K. L. Chan, J. Driscoll, R. D. Sacks, K. D. Wise, S. W. Pangad and E. T. Zellers, *Lab Chip*, 2005, **5**, 1123–1131.
21 J. J. Whiting, C.-J. Lu, E. T. Zellers and R. D. Sacks, *Anal. Chem.*, 2001, **73**, 4668–4675.
22 C.-J. Lu, W. H. Steinecker, W.-C. Tian, M. C. Oborny, J. M. Nichols, M. Agah, J. A. Potkay, H. K. L. Chan, J. Driscoll, R. D. Sacks, K. D. Wise, S. W. Pangad and E. T. Zellers, *Lab Chip*, 2005, **5**, 1123–1131.
23 E. C. Apel, A. J. Hills, R. Lueb, S. Zindel, S. Eisele and D. D. Riemer, *J. Geophys. Res.*, 2003, **108**, 8794–8815.
24 J. A. Syage, B. J. Nies, M. D. Evans and K. A. Hanold, *J. Am. Soc. Mass Spectrom.*, 2001, **12**, 648–655.
25 O. Reynolds, *Philos. Trans. R. Soc. London*, 1879, **170**, 727–845.
26 N. K. Gupta and Y. B. Gianchandani, *Appl. Phys. Lett.*, 2008, **93**, 193511.
27 N. K. Gupta and Y. B. Gianchandani, *Microporous Mesoporous Mater.*, 2011, **142**, 535–541.
28 J. C. Maxwell, *Philos. Trans. R. Soc. London*, 1879, **170**, 231–256.
29 E. Kennard, *Kinetic Theory of Gases*, McGraw Hill, New York, 1938.
30 L. Loeb, *The Kinetic Theory of Gases*, McGraw Hill, New York, 1934.
31 A. A. Alexeenko, S. F. Gimelshein, E. P. Muntz and A. D. Ketsdever, *Int. J. Therm. Sci.*, 2006, **45**, 1045–1051.
32 S. McNamara and Y. B. Gianchandani, *J. Microelectromech. Syst.*, 2005, **14**, 741–746.
33 N. K. Gupta and Y. B. Gianchandani, *Microporous Mesoporous Mater.*, 2010.
34 J. Liu, N. K. Gupta, X. Fan, K. D. Wise and Y. B. Gianchandani, in *Transducer'11*, Beijing, China, 2011, p. M4D.007.
35 G. Serrano, S. M. Reidy and E. T. Zellers, *Sens. Actuators, B*, 2009, **141**, 217–226.
36 J. Liu, Y. Sun and X. Fan, *Opt. Express*, 2009, **17**, 2731–2738.
37 J. Liu, Y. Sun, D. J. Howard, G. Frye-Mason, A. K. Thompson, S.-j. Ja, S.-K. Wang, M. Bai, H. Taub, M. Almasri and X. Fan, *Anal. Chem.*, 2010, **82**, 4370–4375.
38 D. R. Deans and I. M. Scott, *Anal. Chem.*, 1973, **45**, 1137–1141.
39 J. H. Purnell and M. H. Wattan, *J. Chromatogr., A*, 1991, **555**, 173–182.
40 J. R. Jones and J. H. Purnell, *Anal. Chem.*, 1990, **62**, 2300–2306.
41 Y. Sun, J. Liu, D. J. Howard, X. Fan, G. Frye-Mason, S.-j. Ja and A. K. Thompson, *Analyst*, 2010, **135**, 165–171.

